JMEPEG (2004) 13:274-281
DOI: 10.1361/10599490419180

1059-9495/$19.00

Polarization Study on Doped Lanthanum Gallate Electrolyte Using Impedance Spectroscopy

Wenquan Gong, Srikanth Gopalan, and Uday B. Pal

(Submitted 10 November 2003)

Alternating current complex impedance spectroscopy studies were conducted on symmetrical cells of the type [gas, electrode/$La_{1-x}Sr_xGa_{1-y}Mg_yO_3$ (LSGM) electrolyte/electrode, gas]. The electrode materials were slurry-coated on both sides of the LSGM electrolyte support. The electrodes selected for this investigation are candidate materials for solid oxide fuel cell (SOFC) electrodes. Cathode materials include $La_{1-x}Sr_xMnO_3$ (LSM), $La_{1-x}Sr_xCo_yFe_{1-y}O_3$ (LSCF), a two-phase particulate composite consisting of LSM and doped-lanthanum gallate (LSGM), and LSCF + LSGM. Pt metal electrodes were also used for the purpose of comparison. Anode material investigated was the Ni + $Ce_{0.85}Gd_{0.15}O_2$ composite. The study revealed important details pertaining to the charge-transfer reactions that occur in such electrodes. The information obtained can be used to design electrodes for intermediate temperature SOFCs based on LSGM electrolytes.

Keywords anode, cathode, impedance spectroscopy, $La_{1-x}Sr_xGa_{1-y}Mg_yO_3$, solid oxide fuel cells

1. Introduction

Solid oxide fuel cells (SOFCs) offer the possibility of very high-efficiency power generation. They are noiseless, emit far lower quantities of greenhouse gases such as CO_2 compared with conventional power generation systems, and have virtually zero NO_x and SO_x emissions. Despite their many advantages, SOFC power systems are not yet cost-effective enough to merit large-scale deployment in the power generation industry. Of the approaches currently being investigated to decrease the cost of SOFCs, improving power density while decreasing operating temperature is perhaps the most promising option. Improvements in power density will result in decreased system size, which in turn will have the effect of decreasing the size of the balance of plant. Decreasing operating temperature will lead to the deployment of cheaper manifolding and interconnection materials. However, decreasing operating temperature has the effect of increasing all types of polarization losses in the cell. Thus, the simultaneous goals of improving power density while lowering the operating temperature are at odds with each other. Therefore, the focus of recent research has been aimed at the development of more active electrodes and more conductive electrolyte materials that can efficiently operate at lower temperatures (i.e., 600-800 °C).

A very large fraction of the total polarization losses is known to occur at the electrode-electrolyte interfaces, manifesting itself as the kinetic barrier to charge-transfer reactions. Great advances have been made in reducing electrode polarization related to the charge-transfer reaction through the use of two-phase porous composite electrodes[1-4] and mixed conducting electrodes.[5] Much of this work has been aimed at developing electrodes for SOFCs based on the conventional yttria-stabilized zirconia (YSZ) electrolyte. The focus of this article is an investigation of electrode materials for SOFCs based on the perovskite electrolyte $La_{1-x}Sr_xGa_{1-y}Mg_yO_3$ (LSGM). LSGM has received a lot of interest in recent years after it was first reported by Feng and Goodenough[6] to have significantly higher oxygen-ion conductivity than conventional YSZ.

It is generally accepted that high power densities in SOFCs can be achieved only through employment of electrode-supported cells rather than electrolyte-supported cells. There are essentially two options in the design of electrode-supported cells, namely, cathode- and anode-supported SOFCs. Schematics of the two designs are shown in Fig. 1. In both designs, it has been suggested that coarser grained electrodes with coarser connected porosity be used away from the electrolyte-electrode interfaces, while finer grained electrodes with finer connected porosity be used closer to the electrolyte-electrode interfaces. The coarser porosity away from the electrolyte-electrode interface facilitates gas transport, and the finer porosity closer to the interfaces aids in the charge-transfer reactions. This article reports measurements of polarization resistances for various materials near the electrolyte-electrode interface, as shown in Fig. 1. The list of electrode materials investigated in this study is given in Table 1.

Alternating current (AC) complex impedance spectroscopy has been used to measure the effective charge-transfer polarization at the electrode-electrolyte interfaces using symmetrical cell arrangements. The experimental technique is described in the following section.

This paper was presented at the Fuel Cells: Materials, Processing, and Manufacturing Technologies Symposium sponsored by the Energy/Utilities Industrial Sector & Ground Transportation Industrial Sector and the Specialty Materials Critical Technologies Sector at the ASM International Materials Solutions Conference, October 13-15, 2003, in Pittsburgh, PA. The symposium was organized by P. Singh, Pacific Northwest National Laboratory, S.C. Deevi, Philip Morris USA, T. Armstrong, Oak Ridge National Laboratory, and T. Dubois, U.S. Army CECOM.

Wenquan Gong, Srikanth Gopalan, and **Uday B. Pal,** Department of Manufacturing Engineering, Boston University, 15 St. Mary's Street, Boston, MA 02215. Contact e-mail: sgopalan@bu.edu.

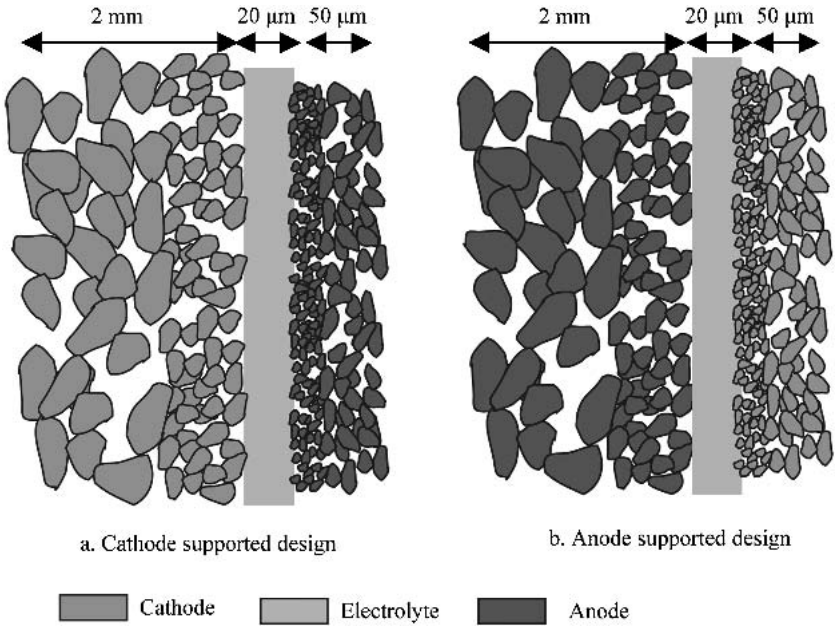

Fig. 1 Schematics of electrode supported SOFCs

Table 1 The List of Electrode Materials Investigated and the Respective Thicknesses

Electrode Materials	Pt	LSM	LSM-LSGM	LSCF	LSCF-LSGM	Ni-GDC
Composition	Pure Platinum	Pure $La_{0.9}Sr_{0.1}MnO_3$	$La_{0.9}Sr_{0.1}MnO_3$ +$La_{0.9}Sr_{0.1}Ga_{0.8}Mg_{0.2}O_3$	Pure $La_{0.6}Sr_{0.4}Co_{0.8}Fe_{0.2}O_3$	$La_{0.6}Sr_{0.4}Co_{0.8}Fe_{0.2}O_3$ +$La_{0.9}Sr_{0.1}Ga_{0.8}Mg_{0.2}O_3$	Ni +$Ce_{0.85}Gd_{0.15}O_2$
Thickness, μm	5	30	30	4.5 ~ 150	30	30

2. Experimental Procedures

2.1 Powder Synthesis

Powders of the composition $La_{0.9}Sr_{0.1}Ga_{0.8}Mg_{0.2}O_3$ (i.e., LSGM) were synthesized by mixing high-purity precursors of lanthanum carbonate, strontium carbonate, gallium oxide, and magnesium oxide in appropriate stoichiometric ratios and calcining them at a temperature of 1200 °C for 4 h in air. Electrode materials such as $La_{0.9}Sr_{0.1}MnO_3$ (LSM), $La_{0.6}Sr_{0.4}Co_{0.8}Fe_{0.2}O_3$ (LSCF), and $Ce_{0.85}Gd_{0.15}O_2$ (GDC) were also made using the same mixing and calcination techniques. The calcined powders were lightly crushed using alumina mortar and pestle, and the calcination step was repeated for completing the solid-state reaction. X-ray powder diffraction analysis confirmed the composition, phase, and purity of the material. All of the synthesized powders (i.e., LSGM, LSM, LSCF, and GDC) and the NiO powder (Baker, Phillipsburg, NJ) were then separately ball-milled in methanol. A laser-scattering particle size distribution analyzer (LA-910, Horiba, Kyoto, Japan) was periodically used at different intervals of the ball-milling process to determine the particle size and distribution. The ball-milling process was stopped when the desired particle size and distribution were obtained. The final particle size and distribution of all the powders are shown in Fig. 2.

2.2 Symmetrical Cell Fabrication

Calcined and milled LSGM powders at room temperature were die-pressed with 10,000 pounds per square inch pressure into pellets and were sintered in air at 1450 °C for 4 h The sintered LSGM pellets were 1.4 mm thick and 2 cm in diameter. The LSGM pellets were then all finely ground to a uniform 1 mm thickness using diamond-grinding discs. LSM-LSGM, LSCF-LSGM, and NiO-GDC composite electrodes were prepared by thoroughly mixing controlled amounts of the powders. The electrode powders (i.e., LSM, LSM-LSGM, LSCF, LSCF-LSGM, and NiO-GDC) each were dispersed in a α-terpeniol solvent to form a paste. The ground LSGM electrolyte pellets were masked with tape to form an outer ring on both sides, and the electrode pastes were painted smoothly on the open circular surfaces. The painted electrolyte pellets were air-dried. The masks were then removed, and the pellets were fired in air for 2 h The firing temperature was 1100 °C for all the cathodic samples and 1300 °C for the anodic samples (i.e., the NiO-GDC electrode). When Pt electrodes were used, commercial Pt paste (6926, Engelhard, East Newark, NJ) was painted over a similarly masked LSGM electrolyte pellet and fired at 950 °C for 2 h All electrodes had the same effective area (~1.33 cm^2). For the cathode materials, Pt mesh was co-sintered onto both electrode surfaces at the same time to act as

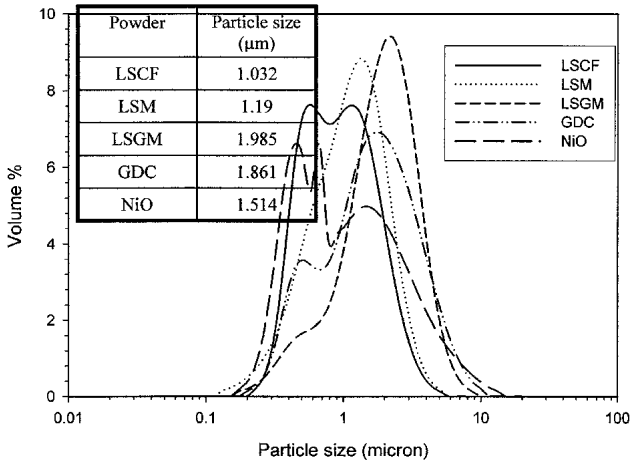

Fig. 2 Final particle size and distribution of the synthesized powders

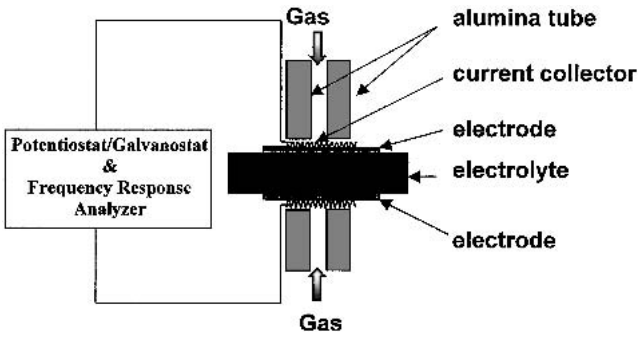

Fig. 3 A schematic diagram showing the measurements

current collectors. Lead wires of Pt were used to connect the Pt mesh current collectors to the AC impedance spectrometer. For the anode materials, Ni mesh was pressed over the electrode surfaces in a reducing atmosphere, and lead wires of Ni were used to connect the current collectors to the spectrometer.

2.3 AC Impedance Characterization

The experimental setup that was used is shown in Fig. 3. In this setup, the symmetrical cell was exposed to the same oxidizing (cathodic) or reducing (anodic) atmosphere on both sides, and a two-probe configuration was used to measure the impedance spectra. During measurement, a constant flow rate of air was maintained for experiments involving the cathode materials, and a constant flow rate of forming gas (i.e., 95% Ar-5% H) was bubbled through water at 25 °C for experiments involving the anode materials. The measurements were made by applying a small-amplitude AC voltage (10 mV) to the cell and monitoring the response current as a function of the AC frequency (from 1 mHz to 65 kHz). A plot of the imaginary part of the measured impedance versus the real part reveals details of the individual ohmic and polarization contributions to the total resistance of the cell. Impedance measurements were made in the temperature range of 600-800 °C in 50 °C increments for all the samples using a potentiostat/galvanostat (263A, Perkin-Elmer, Boston, MA) and an analytical frequency response analyzer (model 1250, Solartron, Houston, TX).

These impedance measurements were performed both as a function of composition for LSM-LSGM electrodes and as a function of electrode thickness for the LSCF electrodes. After electrochemical testing, the samples were epoxy-mounted and polished in cross-section. Both scanning electron microscope (SEM) and optical microscope microscopy were used to measure the grain size, porosity, and thickness of the electrodes, and to confirm the consistency of the microstructure.

3. Results and Discussion

3.1 Microstructure

Typical SEM pictures of the fracture surface of the LSM, LSM-LSGM, LSCF, and LSCF-LSGM electrodes and of their interfaces with the electrolyte are shown in Fig.4. The cross sections in Fig. 4 show that these electrodes have similar microstructures in terms of their interfacial adherence with the LSGM electrolyte, porosity, and grain size. The backscattered SEM pictures of epoxy-mounted and polished LSM, LSM-LSGM, and LSCF electrodes are shown in Fig. 5. The grain size is on the order of 1-2 μm, and the porosity of the LSM, LSM-LSGM, and LSCF electrodes are 55.5%, 54.3%, and 53.3%, respectively, as measured in terms of the percentage area of the pores in the micrographs. Based on the porosity measurement, gas diffusion is not expected to control the polarization process, particularly for the small applied potentials that were used for the AC impedance measurements.

3.2 Impedance Spectroscopy

A typical impedance plot using the symmetrical cell arrangement with LSCF electrodes is shown in Fig. 6. As discussed by previous workers,[7-13] the high-frequency intercept of the impedance spectrum gives the ohmic resistance of the cell (R_s), which includes the resistive contributions of the electrolyte, the two electrodes, the current collectors, and the lead wires. The low-frequency intercepts give the total resistance ($R_s + R_p$), which includes the ohmic resistance of the cell, the concentration polarization (or mass transfer polarization) resistance, the effective charge-transfer polarization resistance (R^{eff}_{ct}), and any other type of polarization resistance arising from adsorption effects. The total polarization resistance of the electrode (R_p) is then extracted from the impedance plot. For all samples measured in this investigation, a single depressed arc was observed. Given that the electrodes were thin, the amplitude of the applied AC voltage was small (10 mV), and the airflow over the electrode was continuous, it is most likely that the effective charge transfer resistance (R^{eff}_{ct}) dominates the polarization resistance for the electrodes. That is, the concentration polarization is negligibly small, and R_p is essentially equal to R^{eff}_{ct}.

3.3 Effect of Cathodic LSM-LSGM Electrode Composition on Polarization Resistance

The typical AC impedance spectra of LSM-LSGM/LSGM/LSM-LSGM symmetrical cells (about 30 μm thickness) tested

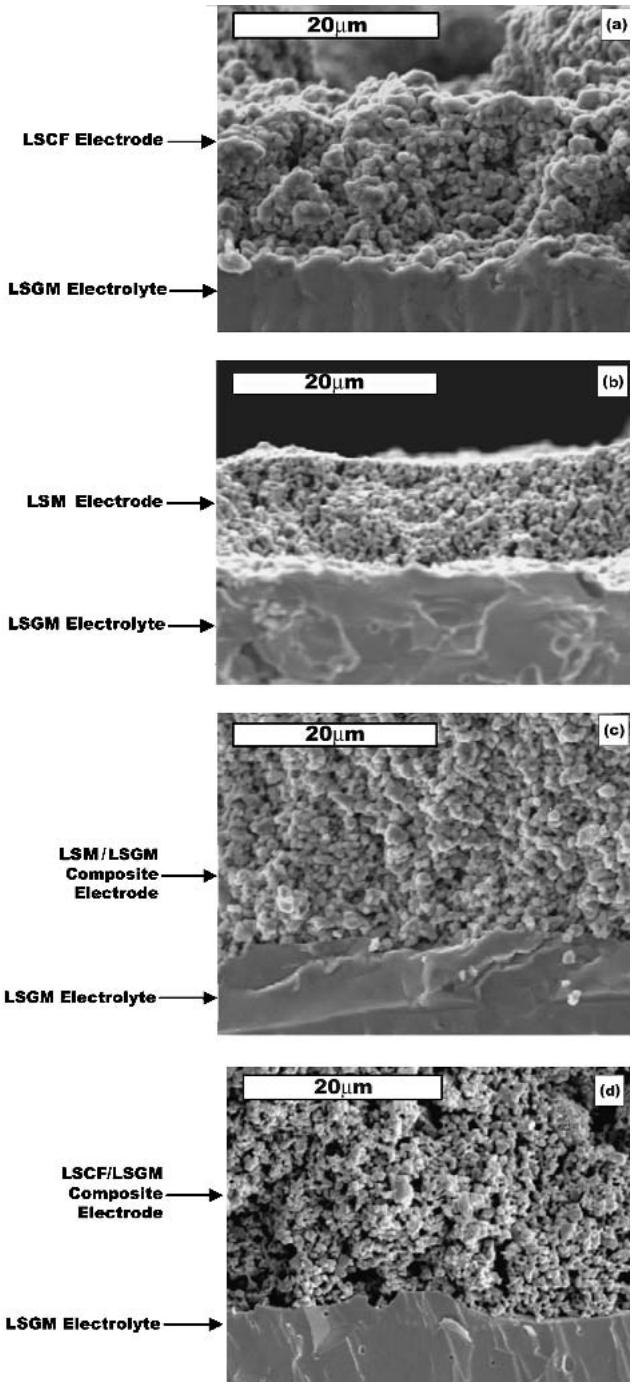

Fig. 4 SEM micrographs of fracture surfaces of (**a**) LSCF/LSGM interface, (**b**) LSM/LSGM interface, (**c**) LSM-LSGM/LSGM interface, and (**d**) LSCF-LSGM/LSGM interface

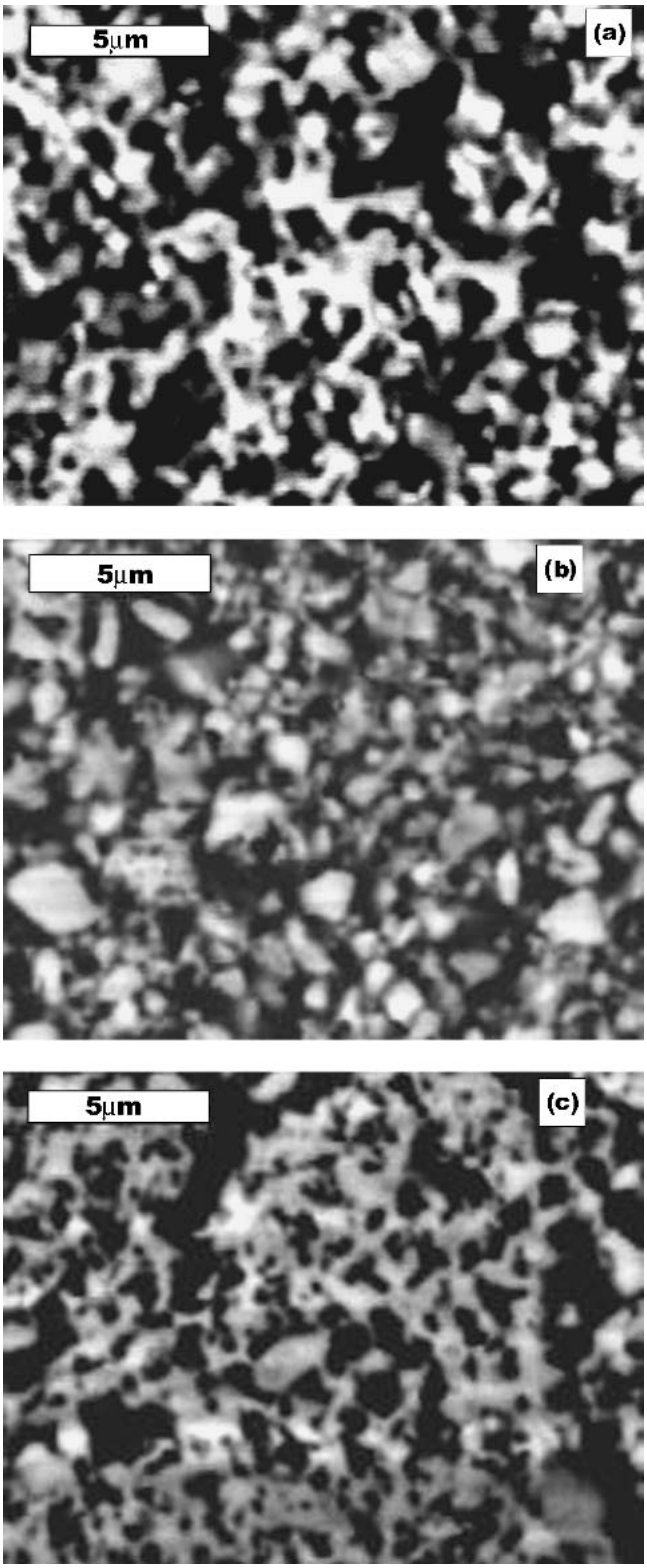

Fig. 5 Backscattered SEM micrographs of polished surfaces of (**a**) LSM electrode, (**b**) LSM-LSGM electrode, and (**c**) LSCF electrode

at 800 °C in air is shown in Fig. 7. It is evident from this figure that when the LSGM content in the electrode was below 70 wt.%, the high-frequency intercepts remained the same, indicating that the effective composite electrode-electrolyte interfacial contact area is roughly equivalent. However, an increase in the LSGM content resulted in a decrease of the polarization resistance, which was due to the increased mixed conducting three-phase boundary (TPB) area within the electrode. When the LSGM content was more than 70 wt.%, which is the percolation threshold, the ohmic resistances of the electrodes were no longer negligible, and therefore the high-frequency intercept

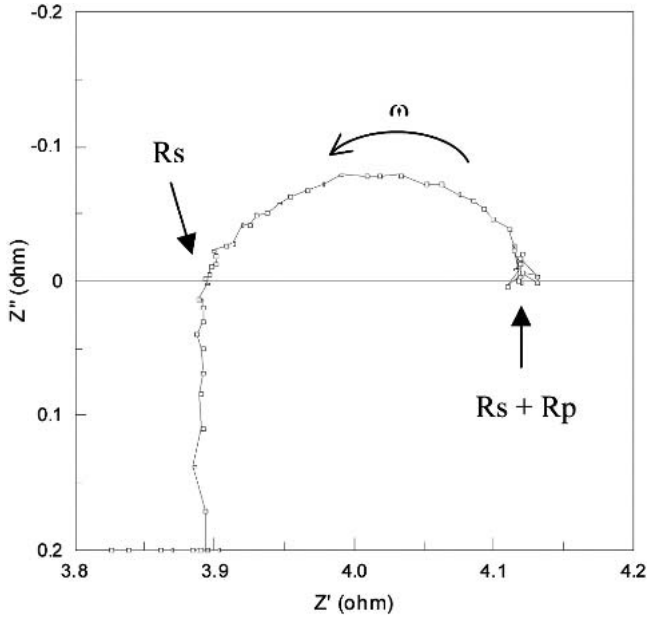

Fig. 6 A typical impedance of symmetrical LSCF/LSGM/LSCF cell in air at 800 °C

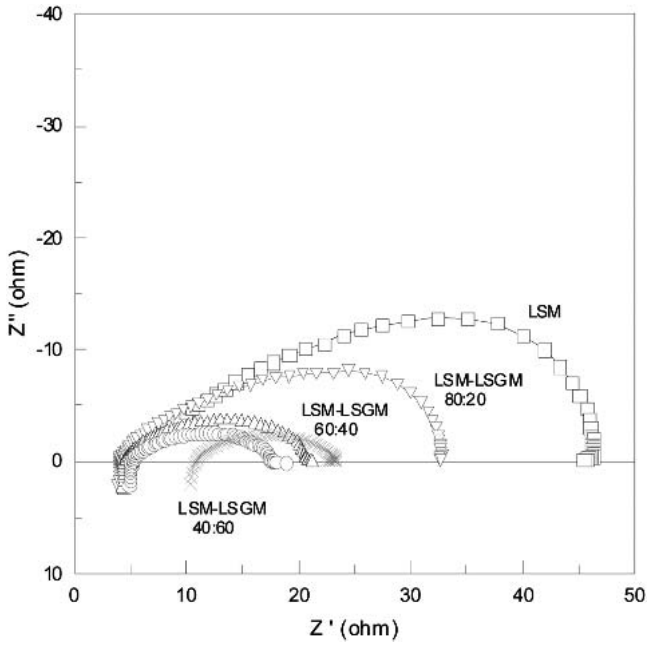

Fig. 7 Typical impedance spectra of symmetrical LSM-LSGM/LSGM/LSM-LSGM cells with different LSM-LSGM compositions measured in air at 800 °C

of the impedance spectra was much larger (Fig. 7). The temperature dependence of the polarization resistance for different LSM-LSGM compositions is shown in Fig. 8. The activation energies as a function of the LSM-LSGM composition obtained from Fig. 8 are shown in Table 2. The activation energies increased with the LSGM content, from 126 kJ/mol for pure LSM to 182 kJ/mol for the 40/60 LSM-LSGM electrode.

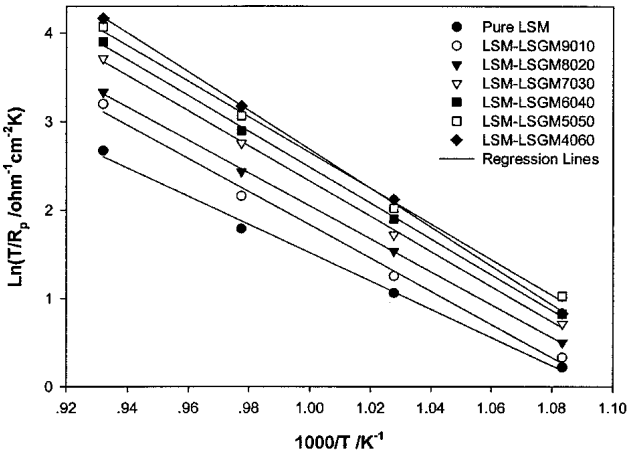

Fig. 8 Temperature dependence of the polarization resistance for different LSM-LSGM compositions measured in air

Table 2 Activation Energies of LSM-LSGM Composite Electrodes on LSGM Electrolytes

	Pure LSM	LSM-LSGM (90:10)	LSM-LSGM (80:20)	LSM-LSGM (70:30)	LSM-LSGM (60:40)	LSM-LSGM (50:50)	LSM-LSGM (40:60)
Ea, kJ/mol	126	156	155	165	168	167	182

This finding suggested that conduction in the composite electrode became more ionic in character as the LSGM content was increased, and resulted in a lowering of the polarization resistance of the electrode within the percolation threshold.

3.4 Effect of Electrode on Cathodic Polarization Resistance

The Arrhenius plot of the measured polarization resistances for the various cathode materials in Table 1 are shown in Fig. 9. It should be noted that the ohmic resistance (R_s) obtained from the high-frequency intercept of the impedance spectra was approximately the same for all of these electrodes, indicating that the effective electrode-electrolyte interfacial contact areas were similar. As can be seen in Fig. 9, the standard 30 μm thick LSM cathode had a polarization resistance that was worse than that of the 5 μm thick Pt electrode. The 30 μm LSM-LSGM (40:60) composite electrode had a polarization resistance that was very similar to that of the Pt electrode. In contrast, the 30 μm thick LSCF electrode had a polarization resistance that was six orders of magnitude lower than the Pt, LSM, and LSM-LSGM electrodes. For the 30 μm LSCF-LSGM (50:50) composite electrode, the polarization resistance was slightly smaller than that of the pure 30 μm LSCF electrode. This can be rationalized on the premise that single-phase LSCF already has a high ionic conductivity. However, adding LSGM to the LSCF electrode can buffer the thermal expansion coefficient of the electrode and bring it closer to the LSGM electrolyte material. The activation energies of these electrodes are listed in Table 3. These values suggest that both the catalytic behavior and the ionic conductor constituent of the electrodes influence the activation energies.

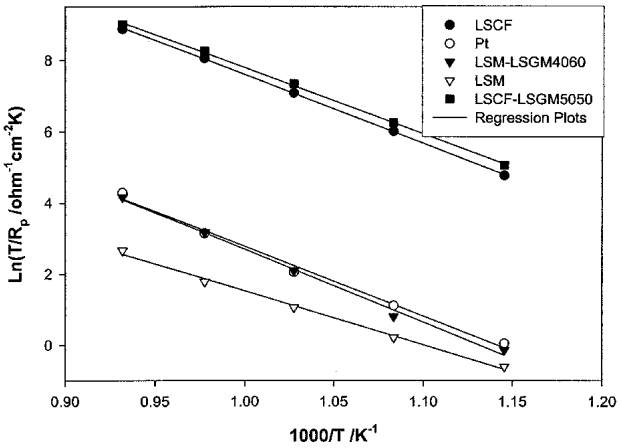

Fig. 9 Temperature dependence of the polarization resistance for various cathode materials measured in air

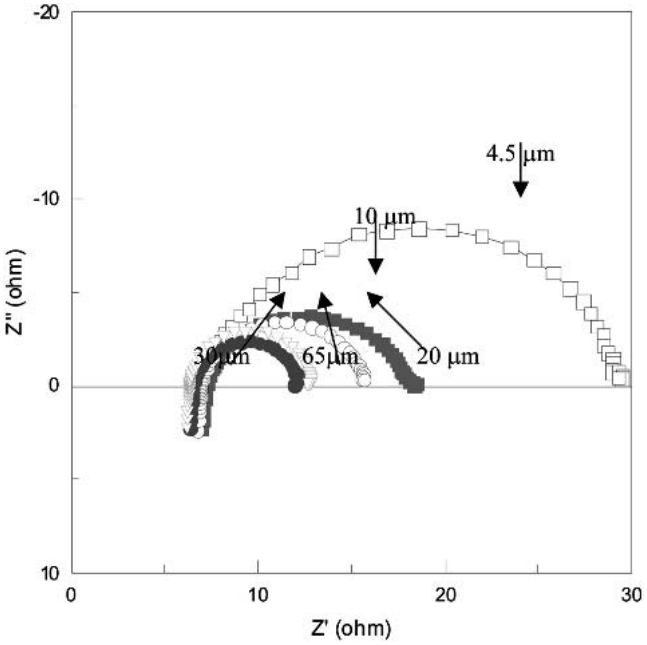

Fig. 10 Impedance spectra of symmetrical LSCF/LSGM/LSCF cells with various electrode thickness measured in air at 600 °C

Table 3 Activation Energies of Investigated Cathodes on LSGM Electrolytes

	Pure LSM	LSM-LSGM (40:60)	Platinum	LSCF	LSCF-LSGM (50:50)
Ea, kJ/mol	126	182	163	165	154

3.5 Effect of LSCF Electrode Thickness on the Effective Charge-Ttransfer Resistance

AC impedance spectra of LSCF/LSGM/LSCF symmetrical cells at 600 °C as a function of electrode thickness are shown in Fig. 10. All the impedance arcs, as stated earlier, appear to be semicircular in nature, and the polarization resistance changed with the thickness of the electrodes. It is evident from Fig. 10 and 11 that increasing the electrode thickness had the effect of decreasing the effective charge-transfer resistance. A similar thickness effect has been observed previously by Kenjo and coworkers[2,14], Tanner et al.[15], and Virkar et al.[16] Tanner et al.[15] developed a comprehensive model to explain the thickness effect of the effective charge-transfer resistance of LSM-YSZ composite electrodes on YSZ electrolytes. When the electrocatalyst cathode is a pure electronic conductor like LSM, the sites for charge-transfer reactions have been conclusively shown by Horita et al.,[17] using oxygen-18 isotope and secondary ion mass spectrometry, to be the TPBs formed between the electrode (i.e., LSM), electrolyte (i.e., YSZ), and the gas phase. Thus, in the case of a porous composite electrode comprising an electrocatalyst phase (LSM), and an ionic conducting phase (YSZ), it is reasonable to expect that increasing the electrode thickness should lead to an increase in the TPB line length and, therefore, to a decrease in the effective charge-transfer resistance. This effective charge-transfer resistance should eventually approach an asymptotic minimum. Indeed, the experimental and theoretical work of Tanner et al.[15] and Virkar et al.[16] showed just such a thickness effect.

In the case of a single-phase mixed ionic and electronic conducting (MIEC) electrode, in addition to the TPBs at the electrode-electrolyte interface, oxygen exchange can occur over the entire pore surface area of the electrode. The nature of this oxygen exchange, whether it is electrochemical (charge-transfer) or simply a chemical exchange process, has been the subject of much recent debate.[18,19] The results presented here do not clarify this debate. However, regardless of the nature of the oxygen exchange process, an increase in MIEC electrode thickness should reduce the total polarization resistance by increasing the number of sites available for exchange between the gas phase and the electrode-electrolyte system, just as in the case of porous composite electrodes.[15] As can be seen from Fig. 11, this is indeed observed for the LSCF/LSGM/LSCF symmetrical cells. Figure 11 also shows a fit to the data using the model developed by Tanner et al.[15] using the following values: porosity (53.3%); intrinsic charge transfer resistance (R_{ct} = 3.8 Ω-cm^2); ionic conductivity (0.025 s/cm); and grain size (1 μm). This also confirms the initial hypothesis that concentration polarization is a minor contributor to the total polarization resistance. Upon increasing the electrode thickness further, pore diffusion of molecular oxygen through the MIEC electrode phase may become rate controlling and, therefore, may increase the total electrode polarization resistance. Indeed, this effect was predicted by Tanner et al.[15] However, such an increase in R^{eff}_{ct} was not observed in the electrode thickness range investigated in this study (4.5-150 μm). This again supports the hypothesis that the electrodes investigated in this study were not "rate-controlled" by gas-phase pore diffusion.

The effect of microstructure changes on effective charge-transfer resistance has not been investigated in this study. It is expected that an electrode with a finer microstructure can lead to a lower effective charge-transfer resistance due to the availability of a greater number of sites for charge-transfer reactions. As shown theoretically by Tanner et al.[15] the thickness at which the asymptotic minimum in the effective charge-transfer resistance is attained for a given electrode depends on the microstructure of the electrode. That is, the finer the elec-

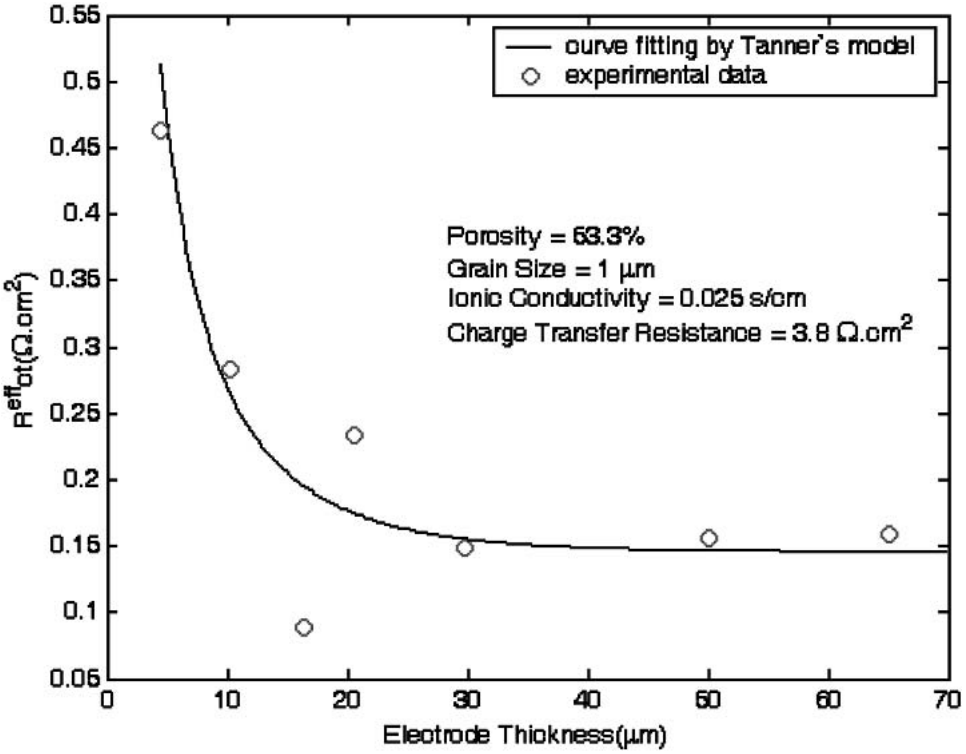

Fig. 11 A plot of charge transfer resistance as a function of electrode thickness for symmetrical LSCF/LSGM/LSCF cells measured in air at 800 °C

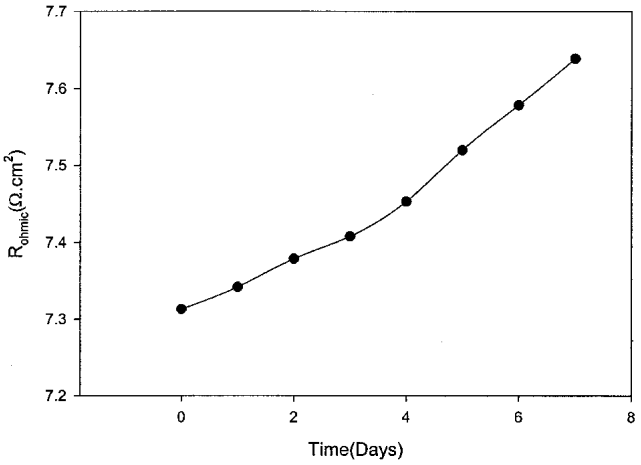

Fig. 12 Time dependence of ohmic resistance of a symmetrical Ni-GDC/LSGM/Ni-GDC cell measured in a reducing atmosphere at 800 °C

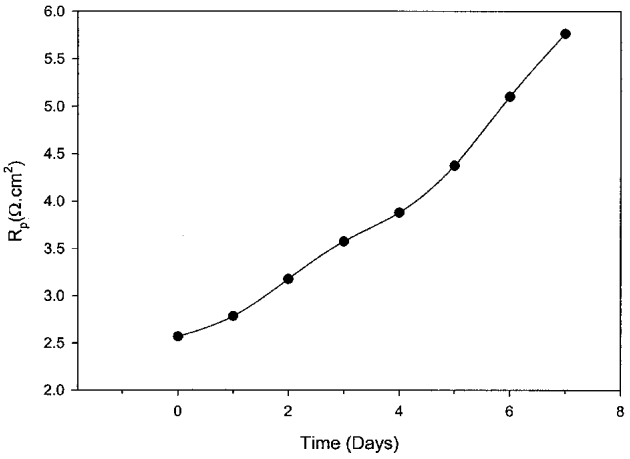

Fig. 13 Time dependence of polarization resistance of a symmetrical Ni-GDC/LSGM/Ni-GDC cell measured in a reducing atmosphere at 800 °C

trode microstructure, the smaller the electrode thickness at which the asymptotic minimum is attained. This behavior will also be dependent on the mixed conducting characteristics of the electrode.

3.6 Effect of Alternate Transport Paths on Effective Charge-Transfer Resistance

In the model developed by Tanner et al.[15] for two-phase composite electrodes (e.g., LSM-YSZ), it has been assumed that the charge-transfer process occurs at the TPBs at the interfaces between the electrode, the electrolyte, and the gas phase. In their calculations, Tanner et al.[15] replaced the TPBs by a negligibly thin continuous region where charge transfer occurs. One of the assumptions in their model is that once oxygen ion formation occurs at the TPBs, the only path for transporting the ions through the contiguous electrolyte grains extends into the electrode. While this may be true in some cases, alternate transport paths for the oxygen ions (e.g., ambipolar surface transport in the MIEC electrodes) may also be

possible and should be considered. Presently, the model by Tanner et al.[15] is being expanded to incorporate such alternate transport paths.

3.7 Effect of Reaction Between Ni Anode Material and LSGM Electrolyte on Polarization Resistance

Nickel is a well-known SOFC anode material, and it acts as the fuel side electrocatalyst and current collector. A Ni-GDC cermet anode is known to be an effective anode for SOFCs based on the LSGM electrolyte.[20] However, upon maintaining a Ni-GDC/LSGM/Ni-GDC symmetrical cell in the same reducing atmosphere at 800 °C, both the ohmic and polarization resistances increased gradually with time, as shown in Fig. 12 and 13. These results confirm prior results[21] that Ni reacts with LSGM to form insulating phases (i.e., lanthanum nickelates) at elevated temperatures. GDC is an excellent oxygen ionic conductor, and is chemically and mechanically compatible with the LSGM electrolyte. Thus, an intermediate dense layer of GDC should be used between the LSGM electrolyte and Ni-GDC anode to prevent direct contact between the Ni in the anode and the electrolyte.

4. Conclusion

Charge-transfer polarization of several candidate electrodes for an LSGM electrolyte has been investigated by AC impedance spectroscopy. Among the cathode materials (i.e., LSM, LSM-LSGM, and LSCF), the pure LSM electrode possessed the worst polarization performance. The addition of the LSGM electrolyte to the LSM electrode increased the mixed-conducting boundary with the gas phase and lowered the polarization. Although LSM-LSGM composite electrodes are better than just pure LSM, the performance of the best LSM-LSGM (40:60) electrode was similar to that of Pt. Single-phase, mixed-conducting LSCF electrodes had a much lower polarization resistance than the LSM-LSGM composite electrodes. As expected, the polarization resistance of the LSCF electrode decreased asymptotically as the electrode thickness increased. Although adding the LSGM electrolyte to the LSCF electrode does not improve the cell performance very much, it does buffer the thermal expansion coefficient of LSCF. The Ni anode reacts with the LSGM electrolyte and lowers the overall cell performance, making a dense layer of GDC between LSGM electrolyte and Ni-GDC anode necessary.

References

1. T. Kawada, N. Sakai, H. Yokokawa, M. Dokiya, M. Mori, and T. Iwata: "Characteristics Of Slurry Coated Nickel Zirconia Cermet Anodes for Solid Oxide Fuel Cell," *J. Electrochem. Soc.*, 1990, *137*, pp. 3042-46.
2. T. Kenjo and M. Nishiya: "$LaMnO_3$ Air Cathodes Containing ZrO_2 Electrolyte for High Temperature Solid Oxide Fuel Cells," *Solid State Ionics*, 1992, *57*, pp. 295-302.
3. M.J.L. Østergård, C. Clausen, C. Bagger, and M. Mogensen: "Manganite-Zirconia Composite Cathodes for SOFC: Influence of Structure and Composition," *Electrochim. Acta*, 1995, *40*, pp. 1971-81.
4. V. Dusastre and J.A. Kilner: "Optimisation of Composite Cathodes for Intermediate Temperature SOFC Applications," *Solid State Ionics*, 1999, *126*, pp. 163-74.
5. M.T. Colomer, B.C.H. Steele, and J.A. Kilner: "Structural and Electrochemical Properties of the $Sr_{0.8}Ce_{0.1}Fe_{0.7}Co_{0.3}O_{3-\delta}$ Perovskite as Cathode Material for ITSOFCs," *Solid State Ionics*, 2002, *147*, pp. 41-48.
6. M. Feng, and J.B. Goodenough: "A Superior Oxide-Ion Electrolyte," *Eur. J. Solid State Inorg. Chem.*, 1994, *31*, pp. 663-72.
7. H. Hu and M. Liu: "Interfacial Studies of Solid State Cells Based Electrolytes of Mixed Ionic-Electronic Conductors," *Solid State Ionics*, 1998, *109*(3-4), pp. 259-77.
8. S. Wang, X. Lu, and M. Liu: "Electrocatalytic Properties of LSM-Based Electrodes for Oxygen Reduction," *J. Solid State Electrochem.*, 2002, *6*, pp. 384-90.
9. S.B. Adler: "Mechanism and Kinetics of Oxygen Reduction on Porous $La_{1-x}Sr_xCoO_{3-\delta}$ Electrodes," *Solid State Ionics*, 1998, *111*, pp. 125-34.
10. P. Costamagna, P. Costa, and V. Antonucci: "Micro-Modelling of Solid Oxide Fuel Cell Electrodes," *Electrochim. Acta*, 1998, *43*, pp. 375-94.
11. A. Barbucci, R. Bozzo, G. Cerisola, and P. Costamagna: "Characterisation of Composite SOFC Cathodes Using Electrochemical Impedance Spectroscopy: Analysis of Pt/YSZ and LSM/YSZ Electrodes," *Electrochim. Acta*, 2002, *47*, pp. 2183-88.
12. J.E. Bauerle: "Study of Solid Electrolyte Polarization by a Complex Admittance Method," *J. Phys. Chem. Solids*, 1969, *30*, pp. 2657-70.
13. R. Macdonald, *Impedance Spectroscopy: Emphasizing Solid Materials and Systems*, Wiley, New York, NY, 1987.
14. T. Kenjo, S. Osawa, and K. Fujikawa: "High Temperature Air Cathodes Containing Ion Conductive Oxides," *J. Electrochem. Soc.*, 1991, *138*, pp. 349-55.
15. C.W. Tanner, K.Z. Fung, and A.V. Virkar: "The Effect of Porous Composite Electrode Structure on Solid Oxide Fuel Cell Performance: I. Theoretical Analysis," *J. Electrochem. Soc.*, 1997, *144*, pp. 21-30.
16. A.V. Virkar, J. Chen, C.W. Tanner, and J.W. Kim: "The Role of Electrode Microstructure on Activation and Concentration Polarizations in Solid Oxide Fuel Cells," *Solid State Ionics*, 2000, *131*, pp. 189-98.
17. T. Horita, K. Yamaji, N. Sakai, Y. Xiong, T. Kato, H. Yokokawa, and T. Kawada: "Determination of Proton and Oxygen Movements in Solid Oxides by the Tracer Gases Exchange Technique and Secondary Ion Mass Spectrometry," *Appl. Surf. Sci.*, 2003, *203-204*, pp. 634-38.
18. M. Liu and Z. Wu: "Significance of Interfaces in Solid-State Cells with Porous Electrodes of Mixed Ionic-Electronic Conductors," *Solid State Ionics*, 1998, *107*, pp. 105-10.
19. S.B. Adler, J.A. Lane, and B.C.H. Steele: "Electrode Kinetics of Porous Mixed-Conducting Oxygen Electrodes," *J. Electrochem. Soc.*, 1996, *143*, pp. 3554-64.
20. J.P.P. Huijsmans, F.P.F. Berkel, and G.M. Christie: "Intermediate Temperature SOFC: A Promise for the 21st Century," *J. Power Sources*, 1998, *71*, pp. 107-10.
21. M. Feng, J.B. Goodenough, K. Huang, and C. Milliken: "Fuel Cells with Doped Lanthanum Gallate Electrolyte," *J. Power Sources*, 1996, *63*, pp. 47-51.